Indian Journal of Chemistry
Vol. 57A, Aug-Sept 2018, pp. 1100-1105

Electrochemical impedance spectroscopy study of oxygen evolution reaction on nanosized $CoWO_4$ and $NiWO_4$

V K V P Srirapu, Ajay Kumar, Nirmala Kumari & Ravindra Nath Singh*

Department of Chemistry, Centre of Advanced Study, Institute of Science, Banaras Hindu University, Varanasi 221 005, India

Email: rnsbhu@rediffmail.com

Received 1 May 2018; revised and accepted 23 July 2018

$CoWO_4$ and $NiWO_4$ have been prepared by a co-precipitation method and investigated as electrocatalysts for the oxygen evolution reaction in 1 M KOH by electrochemical impedance spectroscopy. The electrode kinetic parameters such as the electrochemical active surface area, exchange current density, Tafel slope, and the reaction order are determined. Results have shown that the values of the Tafel slope and reaction order obtained from the EIS study excellently match with those determined by dc techniques.

Keywords: Electrochemistry, Electrochemical impedance, Oxygen evolution, Electrode kinetics, Metal tungstates, Tungstates, Cobalt, Nickel

The rapid industrialization, excessive use of fossil fuels and their harmful effects on the environment have drawn much attention towards development of environmental-friendly energy programs wherein the electrical energy is obtained from nonconventional energy sources such as solar energy. As solar energy is intermittently available, it is desirable to develop efficient and low-cost energy conversion and storage devices such as water electrolysis and fuel cells so as to maintain the supply of electrical power produced from the solar energy without any failure. Water electrolysis is the simplest process to store light or electrical energy in the form of a non-pollutant fuel, hydrogen. On demand, hydrogen can easily be transformed into electrical energy through a suitable fuel cell.

Water electrolysis comprises two half-cell reactions: H_2 evolution (HER) and O_2 evolution (OER). The latter is kinetically sluggish and takes place at the anode at much higher over-potentials, compared to the cathodic HER,[1] which has motivated the researchers to discover efficient electrocatalysts[2,3] with significantly reduced oxygen over-potentials. At present, RuO_2 and IrO_2 are the best electrocatalysts for OER,[4,5] however, they are very costly and less abundant on the earth, which restrict their large scale applications. Concerted efforts have already been made to develop efficient, robust and low-cost electrode materials for OER. Among the catalysts investigated, transition metal mixed oxides of spinel (mainly Co-based)[6-10] and perovskite[11-14] families are considered as promising electrode materials for OER in alkaline solutions and have been comprehensively reviewed.[15,16] Recently, a new series of mixed oxides with compositional formulae, $MM'MoO_4$ (where M = Fe, Co or Ni; M′ = Fe, Cr or Ni) have also been reported as OER active and stable materials in alkaline solutions.[17-19]

A survey of literature reveals that the most of studies reported on OER are based on dc techniques such as cyclic (CV) and linear sweep (LSV) voltammetries and Tafel polarization. Very few reports[20-22] are available wherein the electrode kinetic parameters, i.e., the Tafel slope (*b*) and the reaction order (*p*) were obtained by electrochemical impedance technique. Very recently, we have carried out a detailed study of OER on two novel electrode materials, $CoWO_4$ and $NiWO_4$ in 1 M KOH using dc polarization techniques.[23] We have now performed similar studies on the same electrode materials by ac impedance spectroscopy. The latter technique is novel and requires considerably less time for the investigation. Results have shown that *b* and *p* values, obtained from the EIS study agree fairly well with those determined using dc techniques. Detailed results of the investigation are reported in this study.

Materials and Methods

$CoWO_4$ and $NiWO_4$ were prepared by a co-precipitation method.[23] The oxides were characterized structurally by FT-IR, XRD, TEM, XPS, and BET surface area measurements. These catalysts followed the crystalline monoclinic structure with space groups, P2/a (13) and P2/c (13), respectively. The $CoWO_4$ (26–30 nm) and $NiWO_4$ (22–30 nm) nanoparticles (NPs) were nearly spherical. The constituent metals of the oxide, W and Co (or Ni) had oxidation states +6 and +2, respectively. Details of preparation and characterization of the catalytic materials are described elsewhere.[23] The oxide electrode was prepared by dropping the catalyst suspension in ethanol-water (2:1) mixture over the pretreated glassy carbon (GC) electrode surface, as described previously.[23] Loading of each oxide on GC was 0.2 mg cm^{-2}.

Electrochemical impedance spectroscopy (EIS) was performed in a conventional three-electrode-single compartment Pyrex glass cell using a Bio-Logic SAS SP-150. Three electrodes were used: test (catalyst/GC, 0.5 cm^2), counter (pure Pt-foil, ~8 cm^2) and reference (Hg/HgO, OH^- (1 M), E° = 0.098 V versus SHE). All the potentials mentioned in the text are against this reference electrode only. The EIS study of catalysts in 1 M KOH was carried out at the open-circuit-potential (OCP values being –0.051 and –0.061 V for $CoWO_4$/GC and $NiWO_4$/GC, respectively) and at varying potentials (0.58–0.64 V) and KOH concentrations (0.5–2.0 M) in the initial region of OER. The frequency range and ac voltage amplitude employed were 100×10^3–0.05 Hz and $\pm$5 mV, respectively. Prior to impedance measurements, the catalyst electrode was equilibrated to each applied potential for 300 s. To make the contribution of the counter (Pt) electrode negligible to the measurement of the overall cell impedance, the geometrical area of the electrode was kept considerably large (~16 times). The software 'ZsimpWin' version 3.00 was used to analyze the impedance parameters.

Results and Discussion

To determine the electrochemical and electrode kinetic parameters such as the electrochemically active surface area (EASA), solution resistance (R_s), the charge transfer resistance (R_{ct}), the Tafel slope (b), the reaction order (p), etc., the EIS study of electrocatalysts has been performed at varying potentials in 1 M KOH and at varying KOH concentrations at a constant potential. Results of the investigation are described below.

Electrochemically active surface area (EASA)

For comparison of electrocatalytic activities, the determination of electrochemically active surface area (EASA)/roughness factor (R_f) of the catalyst electrodes is desired. The EASA of the catalyst has been determined with the help of the double layer capacitance (C_{dl}) of the catalyst/1 M KOH interface using the relation,[23]

R_f = obs. C_{dl} of the catalyst electrode/C_{dl} of the smooth carbon material per unit area (i.e., 20 μF cm^{-2}) in alkaline solution.

The C_{dl} of the catalyst was determined by electrochemical impedance spectroscopy (EIS). EIS measurements on the catalyst/1 M KOH system have been made in the potential region $\pm$0.050 V centered at the OCP. The frequency range employed was between 100 kHz and 50 Hz. The higher frequency range 100 kHz and 50 Hz was chosen so as to make the contributions of other processes, such as ion adsorption, intercalation, etc., negligible toward the measured capacitance.[24]

Results of EIS in Nyquist mode are represented in Fig. 1. Features of Nyquist curves appear to be similar, showing only one time constant. The experimental data were, therefore, analyzed using electrical equivalent circuit, R_s (R_p Q_{dl}), where R_s and R_p are the solution and polarization resistances and Q_{dl} is the constant phase element (CPE) related to the double layer capacitance (C_{dl}). CPE can be defined as[24] $Z_{CPE} = 1/[Q\ (j\omega)^{1-\alpha}]$, where Z_{CPE} is the impedance of the CPE. α is an exponent ($\alpha \leq 1$) which is equal to unity in the case of an ideal capacitor with $Q = C_{dl}$, and equal to zero when CPE describes an ideal resistor with $Q = R$. Moreover, the exact physical interpretation of the CPE is not very clear. Based on the proposed equivalent circuit model, simulated and experimental curves tally fairly well as shown in Fig. 1. Estimates of the circuit parameters shown in Table 1 are averages of three electrodes of each catalyst. In Table 1, values of α are close to 1 and therefore Q can be assumed to be the C_{dl} of the catalyst/1 M KOH interface. Thus, C_{dl} (= observed C_{dl} of the electrode/geometrical area of the same electrode) of $CoWO_4$ and $NiWO_4$ electrodes are 20.9 and 22.9 μF cm^{-2}. However, values of C_{dl} determined by the cyclic voltammetry method were ~38.0 and ~25.6 μF cm^{-2} for $CoWO_4$ and $NiWO_4$, respectively.[23]

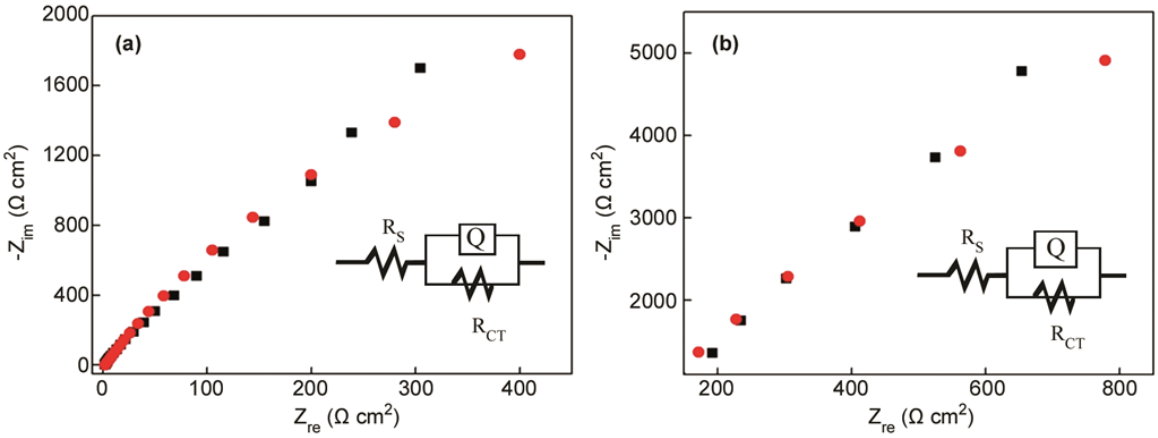

Fig. 1 — Nyquist curves (experimental and simulated) for (a) $CoWO_4$, and, (b) $NiWO_4$ films on GC at the open-circuit potential in 1 M KOH at 298K. [Geometrical area of the catalyst electrode: 0.5 cm^2; mass of the catalyst film: 0.2 mg cm^{-2}].

Table 1 — Impedance measurements on $CoWO_4$ and $NiWO_4$ films on GC at the open-circuit potential in 1 M KOH. [Geometrical area of the catalyst electrode: 0.5 cm^2, mass of the catalyst film: 0.2 mg cm^{-2}, frequency range: 10^5 –10 Hz, Temp.: 298 K]

Parameter	$CoWO_4$/GC	$NiWO_4$/GC
R_s (Ω cm^2)	2.4	2.9
$10^6 Q_{dl}$ (Ω^{-1}s^n cm^2)	10.43±0.34	11.43±0.11
α	0.92±0.01	0.92±0.00
R_p (Ω cm^2)	1.876±0.078×10^4	12.36±4.92×10^{12}
R_f (Ω cm^2)	1.0	1.1

The higher C_{dl} values obtained by the cyclic voltammetry method can be ascribed to some contribution of faradaic processes during measurements of charging and discharging curves. In fact, cyclic voltammetry gives reasonably good results in the case of porous oxide electrodes with reasonably large roughness factors.

Electrode kinetic study

To determine the Tafel slope, EIS measurements were made on the catalyst electrode in 1 M KOH at four different potentials, 0.580, 0.600, 0.620 and 0.640 V in the initial region of OER. Features of Nyquist curves for $CoWO_4$ and $NiWO_4$ at varying potentials (shown in Fig. 2) were similar. Each curve exhibited a depressed semicircle over the frequency range (100 kHz–50 mHz) employed in the study. It was observed that the diameter of the semicircle decreased with increasing potential. This demonstrates that the depressed semicircle originates from the OER.

To analyze the experimental impedance data, we have employed a common equivalent circuit, R_s (Q_1 (R_1 (Q_2 R_2))), which is similar to those recently

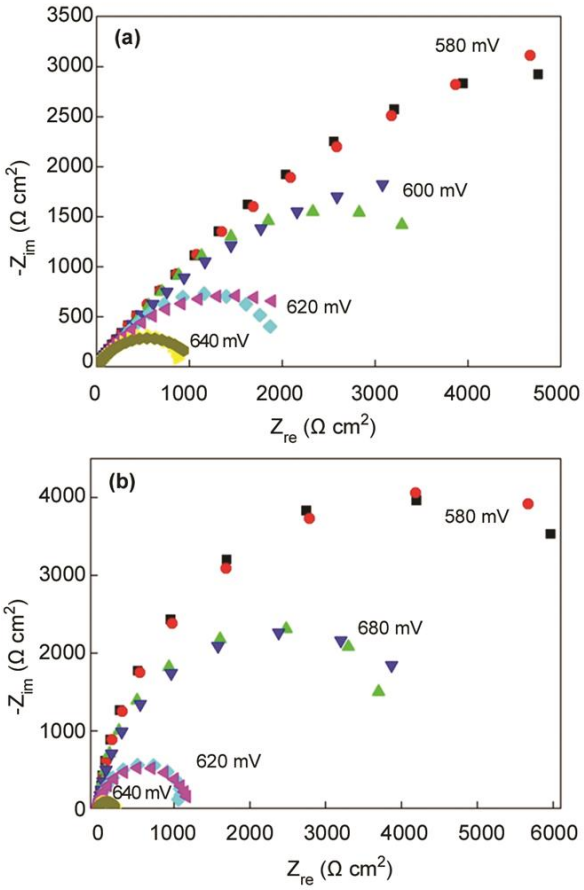

Fig. 2 — Nyquist curves (experimental and simulated) for (a) $CoWO_4$, and, (b) $NiWO_4$ films on GC at varying potentials in 1 M KOH at 298 K. [Geometrical area of the catalyst electrode: 0.5 cm^2; mass of the catalyst film: 0.2 mg cm^{-2}].

employed by Swierk *et al.*[22] and Lyons and Brandon[25] in the OER study. R_s is the uncompensated solution resistance, and Q_1 is the constant phase element related to the double layer capacitance. The circuit

elements, R_1, R_2 and Q_2 have been used to take into account the faradaic OER. The polarization resistance, R_1, is related to the overall rate of the OER and incorporates the charge transfer resistances[22,25] of the various steps involved within the OER including the rate determining step. R_2 is related to the ease with which one or more surface intermediates are formed. The sum, 'R_1 + R_2', gives the faradaic resistance (R_F) of the catalyst.[25,26] The circuit component, (Q_2 R_2) models the relaxation of the charge associated with the formation of surface adsorbed intermediates. Contributions of the film resistance and capacitance, in the employed frequency window, toward the measured cell impedance being negligible, the loop related to the catalytic film has been excluded from the proposed equivalent circuit model.

It is observed that simulated EIS data, based on the proposed equivalent circuit model, agrees fairly well with the experimental data. Simulated EIS data in Nyquist mode in the case of $CoWO_4$ and $NiWO_4$ films are shown in Fig. 2. Estimates of the circuit parameters are given in Table 2.

The variation of R_F as a function of the applied potential is represented in Fig. 3. This figure indicates that R_F decreases, and hence the rate of OER increases with increasing the applied potential on both the catalytic films.

The Tafel slopes (b) are normally determined by recording dc steady-state Tafel polarization curves and measuring their slopes in the Tafel region where j is related to η via the following expression:

$$j = j_o \exp[2.303\ \eta/b] \quad \ldots (1)$$

Differentiating j with respect to η gives Eq. (2)

$$dj/d\eta = 2.303\ j_o/b \exp[2.303\eta/b] \quad \ldots (2)$$

Taking log of Eq. 2 gives Eq. (3)

$$\log(dj/d\eta) = \log(2.303\ j_o/b) + \eta/b \quad \ldots (3)$$

Table 2 — Impedance circuit parameters for OER on $CoWO_4$ and $NiWO_4$ films on GC in 1 M KOH at 298 K. [Geometrical area of the catalyst electrode: 0.5 cm^2, mass of the catalyst film: 0.2 mg cm^{-2}]

Potential (V)	$R_{-\Omega}$ (Ω cm^2)	$10^6 Q_1$ ($\Omega^{-1}s^n$ cm^2)	$\alpha 1$	R_1 (Ω cm^2)	$10^5 Q_2$ ($\Omega^{-1}s^n$ cm^2)	$\alpha 2$	$10^{-3} R_2$ (Ω cm^2)	$R_F = (R_1 + R_2)$ (Ω cm^2)
				$CoWO_4$/GC				
0.58	2.09	5.39	0.970	1.13	24.81	0.538	17.80	17801.13
0.60	1.75	87.58	0.755	226.20	25.45	0.605	5.93	6156.20
0.62	1.80	112.20	0.746	179.70	27.07	0.668	2.24	2419.70
0.64	1.84	138.90	0.740	123.80	27.91	0.717	0.87	993.80
				$NiWO_4$/GC				
0.58	2.56	20.89	1.0	16.41	6.067	0.911	9.023	9039.41
0.60	2.53	25.22	1.0	13.20	7.391	0.917	4.963	4976.20
0.62	2.50	24.87	1.0	10.79	9.303	0.876	1.283	1293.79
0.64	2.43	20.34	1.0	6.62	15.330	0.789	0.227	233.62

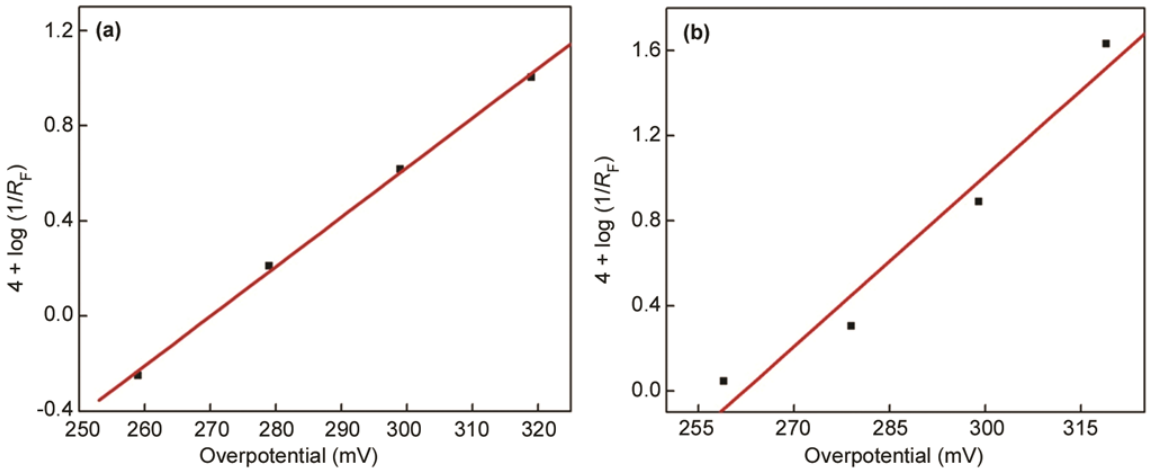

Fig. 3 — Plots of log (1/R_F) versus overpotential for (a) $CoWO_4$, and, (b) $NiWO_4$. [Geometrical area of the catalyst electrode: 0.5 cm^2; mass of the catalyst film: 0.2 mg cm^{-2}].

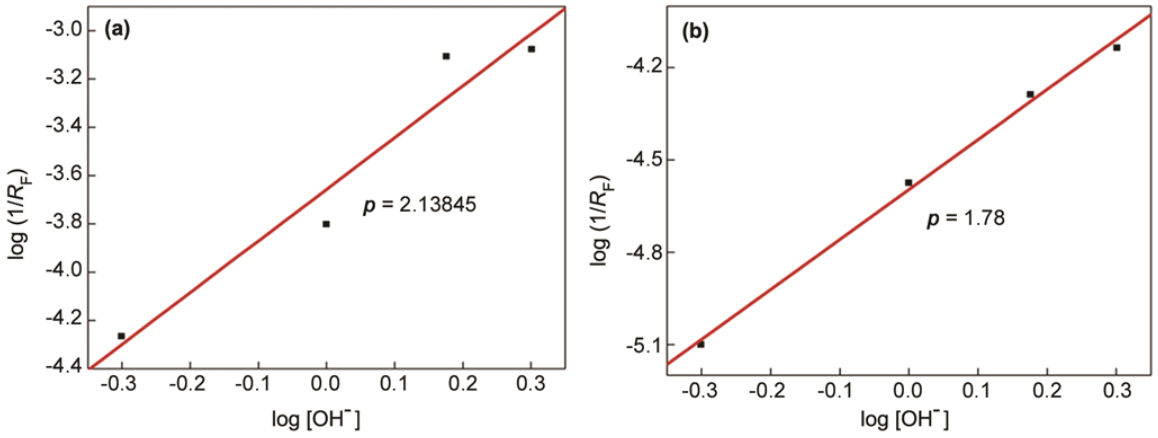

Fig. 4 — Plots of log ($1/R_F$) versus log C_{OH^-} for (a) $CoWO_4$, and, (b) $NiWO_4$. [Geometrical area of the catalyst electrode: 0.5 cm^2, mass of the catalyst film: 0.2 mg cm^{-2}].

Table 3 — Circuit parameters for OER on $CoWO_4$ and $NiWO_4$ at E = 0.60 V at varying KOH concentrations at 298 K

[KOH] (M)	R_s (Ω cm^2)	$10^5 Q_1$ (Ω^{-1} s^n cm^2)	$\alpha 1$	R_1 (Ω cm^2)	$10^4 Q_2$ (Ω^{-1} s^n cm^2)	$\alpha 2$	R_2 (Ω cm^2)	R_F (Ω cm^2)
				$CoWO_4$/GC				
0.5	5.03	5.408	0.85	10140	2.795	0.904	8242	18382
1.0	2.12	18.58	0.72	6.892	19.24	0.979	6322	6328.89
1.5	1.47	21.87	0.73	5.279	3.50	0.721	1274	1279.28
2.0	1.38	46.93	0.70	1.358	12.74	0.676	1196	1197.36
				$NiWO_4$/GC				
0.5	4.23	2.15	0.917	110100	3.38	1.0	15940	126040
1.0	2.23	1.72	0.933	60	2.96	0.915	37480	37540
1.5	1.77	2.09	0.926	13510	0.120	0.935	5935	19450
2.0	1.10	2.29	0.928	7200	0.103	1.0	6452	13650

As $dj/d\eta = 1/R_F$, where R_F is the Faradaic resistance, Eq. 3 becomes

$$\log (1/R_F) = \eta/b + \log (2.303\, j_o/b) \quad \ldots (4)$$

Equation 4 demonstrates that the plot of $\log(1/R_F)$ versus overpotential produces a straight line (Fig. 3), the inverse of slope of which gives the Tafel slope (b = 1/slope). Values of b, thus estimated, were 47.6 and 37.4 mV for $CoWO_4$ and $NiWO_4$ films on GC, respectively. The low Tafel slopes indicate that these oxide catalysts are quite active for OER in alkaline solutions. Similar Tafel slopes were also found for the OER on these oxides through dc Tafel polarization measurements.[23] The exchange current density (j_o) estimated from the intercept of the straight line on the $\log(1/R_F)$ axis at η = 0 was found to be 4.96×10^{-5} and 0.16×10^{-5} for OER on $CoWO_4$ and $NiWO_4$, respectively.

EIS measurements were also carried out at varying KOH concentrations and at a constant potential (E = 0.60 V) chosen in the initial OER region so as to minimize the effect of evolving O_2 bubbles. EIS data, so obtained, are shown in Fig. 4 and results of analyses are given in Table 3. To determine the order, the linear $\log (1/R_F)$ versus $\log C_{OH^-}$ curves were constructed and their slopes were measured. Values of the slope were 1.8 and 1.7 on $CoWO_4$ and $NiWO_4$, respectively. These values are very close to those already found for OER on the same catalyst electrodes, $CoWO_4$ (p = 2) and $NiWO_4$ (p = 1.7)[23] under similar experimental conditions (i.e., [KOH] = 1 M; temp. = 298 K).

Conclusions

The study demonstrates that the electrode kinetic parameters, Tafel slope and the reaction order for the OER determined from the EIS study are very close to those obtained from the steady-state dc polarization techniques. This justifies the suitability of application of ac impedance technique as well as the equivalent circuit model, proposed by Swierk *et al*. for simulation of impedance data in the OER region.

Acknowledgement

We thank the University Grants Commission Govt. of India, New Delhi, for financial support. (F. No. 18-1/2014 BSR and UGC-Res Fellow, BHU-Scheme no. 5012).

References

1 Man I C, Su H Y, Calle-Vallejo F, Hansen H A, Martínez J I, Inoglu N G, Kitchin J, Jaramillo T F, Nørskov J K & Rossmeisl J, *Chem Cat Chem*, 3 (2011) 1159.
2 Gong M, Li Y, Wang H, Liang Y, Wu J Z, Zhou J, Wang J, Regier T, Wei F & Dai H, *J Am Chem Soc*, 135 (2013) 8452.
3 Louie M W & Bell A T, *J Am Chem Soc*, 135 (2013) 12329.
4 Tsuji E, Imanishi A, Fukui K & Nakato Y, *Electrochim Acta*, 56 (2011) 2009.
5 Hu J M, Zhang J Q & Cao C N, *Int J Hydrogen Energy*, 29 (2004) 791.
6 Lal B, Singh N, Samuel S & Singh R N, *J New Mater Electrochem Sys*, 2 (1999) 59.
7 Chi B, Li J, Yang X, Lin H & Wang N, *Electrochim Acta*, 50 (2005) 2059.
8 Laouini E, Hamdani M, Pereira M, Douch J, Mendonça M, Berghoute Y & Singh R N, *Int J Hydrogen Energy*, 33 (2008) 4936.
9 Singh R N, Singh J, Lal B & Singh A, *Int J Hydrogen Energy*, 32 (2007) 11.
10 Lu B, Cao D, Wang P, Wang G & Gao Y, *Int J Hydrogen Energy*, 36 (2011) 72.
11 Tiwari S, Koenig J, Poillerat G, Chartier P & Singh R N, *J Appl Electrochem*, 28 (1998) 114.
12 Tiwari S, Singh S & Singh R N, *J Electrochem Soc*, 143 (1996) 1505.
13 Lal B, Raghunandan M, Gupta M & Singh R N, *Int J Hydrogen Energy*, 30 (2005) 723.
14 M E, Taroˆco H A, Matencio T, Domingues R Z & dos Santos J A, *Int J Hydrogen Energy*, 37 (2012) 6400.
15 Hamdani M, Singh R N & Chartier P, *Int J Electrochem Sci*, 5 (2010) 556.
16 Chen D, Chen C, Baiyee Z M, Shao Z & Ciucci F, *Chem Rev*, 115 (2015) 9869.
17 Singh R N, Awasthi R & Sinha A, *J Solid State Electrochem*, 13 (2009) 1613.
18 Singh R N, Kumar M & Sinha A, *Int J Hydrogen Energy*, 37 (2012) 15117.
19 Srirapu V K V P, Sharma C S, Awasthi R, Singh R N & Sinha A S K, *Phy Chem Chem Phy*, 16 (2014) 7385.
20 Lyons M E & Brandon M P, *J Electroanal Chem*, 631 (2009) 62.
21 Costa F R, Franco D V & Da Silva L M, *Electrochim Acta*, 90 (2013) 332.
22 Swierk J R, Klaus S, Trotochaud L, Bell A T & Tilley T D, *J Phy Chem C*, 119 (2015) 19022.
23 Srirapu V K V P, Kumar A, Srivastava P, Singh R N & Sinha A, *Electrochim Acta*, 209 (2016) 75.
24 McCrory C C, Jung S, Peters J C & Jaramillo T F, *J Am Chem Soc*, 135 (2013) 16977.
25 Lyons M E & Brandon M P, *Int J Electrochem Sci*, 3 (2008) 1386.
26 Doyle R L & Lyons M E, *Phy Chem Chem Phy*, 15 (2013) 5224.